Low Temperature Physics/Fizika Nizkikh Temperatur, 2020, v. 46, No. 8, pp. 920–926

Dipole-dominated dissipative magnetic solitons in quasi-one-dimensional spin-torque oscillators

R.V. Verba

Institute of Magnetism NAS of Ukraine and MES of Ukraine, Kyiv 03142, Ukraine
E-mail: verrv@ukr.net

V.S. Tiberkevich and A.N. Slavin

Department of Physics, Oakland University, Rochester, Michigan 48309, USA

Received March 5, 2020, published online June 22, 2020

It is well-known that a spin-transfer torque caused by a dc electric current can excite in a two-dimensional ferromagnetic film exchange-dominated magnetic solitons, often called “spin-wave bullets”, under the condition of a negative nonlinear shift of spin wave frequency. In this work, we demonstrate that in a quasi-one-dimensional (1D) case, e.g., in a nanowire spin-Hall oscillator, it is possible to excite a stable dissipative magnetic soliton, which is dominated by the dipole-dipole interaction. This dissipative magnetic soliton can be described in the framework of a 1D Ginzburg–Landau auto-oscillator model, and has the shape similar to that of the exchange-dominated spin wave bullet, but with a different spatial localization law. The influence of the dipolar interaction makes possible the stabilization of a dissipative soliton in a relatively large (micron-sized) active area of the oscillator, which is in a sharp contrast with the two-dimensional case, where the excitation of a stable spin-wave bullet was observed only in relatively small active areas having typical sizes of the order of 100 nm. The characteristics and possible applications of these dipole-dominated spin wave bullets are discussed.

Keywords: spin-wave bullet, spin-torque oscillator, soliton, dipolar interaction.

1. Introduction

The inherent nonlinearity of magnetization dynamics, which is, mostly, of a topological origin [1], leads to the possibility of formation of a wide variety of static and dynamic magnetic solitons, which can exist in ferromagnetic samples [2,3]. The pioneering theoretical works describing the conditions of formation and classification of magnetic solitons were performed in 1970th [4–7], followed up by the experimental studies of the spin-wave (SW) envelope solitons in continuous ferrite films [8,9]. Recent progress in the nanopatterning, engineering of magnetic interfaces and multilayers allows for the experimental observation of many kinds of static magnetic solitons, for instance, vortices [10,11], skyrmions [12–15], magnetic bobbers [16], spin meron pairs [17].

An important turning point in the investigations of dynamic magnetic solitons was the discovery of the spin-transfer torque (STT) effect [18,19]. By means of the STT it becomes possible, under certain conditions, to completely compensate magnetic damping [20], and, thus, to realize experimentally highly nonlinear cases of the magnetization dynamics described theoretically in [2,21]. First, it was theoretically predicted [22] and, then, experimentally confirmed [23] that in the case of an in-plane magnetized two-dimensional (2D) ferromagnetic film a local application of STT can lead to the excitation of a particular type of a dynamic magnetic soliton, called a “spin wave bullet”. Later, the excitation by means of STT of the other types of magnetic solitons, such as multibullets [24], droplets [25–27] and dynamic skyrmions [28] was also demonstrated.

The excitation of the SW bullets was extensively studied in the two-dimensional case, when a ferromagnet forming a free layer of a spin-torque oscillator (STO) or a spin-Hall oscillator (SHO) is an extended film, and the STT acts on it locally. In such cases the local STT action (or local injection of a spin current) is created by the use a point contact [23,29] or a current concentrator [30]. The SW bullets can be excited under the condition of a negative nonlinear shift of the SW frequency, which can be realized, e.g., in the case of an in-plane magnetized isotropic ferromagnetic film. In such a case, the frequency of the magnetization oscillations decreases with the increase of the oscillation amplitude, and, at a certain amplitude, goes below the spect-

rum of the linear SWs. This nonlinear transformation of a large-amplitude SW into an evanescent state constitutes a nonlinear self-localization mechanism leading to the formation of a spatially localized SW bullet. In a 2D case the formation of the SW bullets is dominated by the exchange interaction, and is well described within the purely exchange model [22]. The characteristic size of an SW bullet in such a case is determined by the exchange length of a ferromagnetic medium, and, typically, does not exceed 100–200 nm. If one applies an external STT to a much larger area, the coherent excitation of SW bullets (or any other mode) becomes impossible, and, instead, a subthreshold "heating" of many different SW modes is observed [31].

In contrast, in a quasi-1D case taking place, e.g., in a nanowire SHO [32], the coherent single-mode generation was observed in the SHO devices having much larger sizes of the SHO active area (area where the STT in applied) exceeding 1 μm [32,33]. Later, we found [34] that in this case the SW mode excited by the STT is also a nonlinear self-localized SW bullet, but its formation is dominantly affected by the dipole-dipole interaction. It should be noted, that the existence of dipole-dominated bullets is not trivial, as in this 1D geometry the Lighthill criterion [35], necessary for the formation of conservative dynamic solitons is not fulfilled. Thus, these dipole-dominated bullets can be classified as purely dissipative magnetic solitons (see, e.g., [2]), that can exist only in an active, externally pumped medium, like an active area of an SHO. In this work we present a detailed numerical study of such dipole-dominated magnetic solitons, and consider the conditions when the dipolar interaction dominates the formation of the SW bullets.

2. Model of 1D spin-torque oscillator

The most common realization of a quasi-1D case is a SHO based on a bilayer nanowire comprising a ferromagnet and a heavy metal, the sketch of which is presented in Fig. 1. If a nanowire is sufficiently narrow, the profile of the exited SW mode is determined by the lateral quantization and nonuniformity of the static magnetic field across the nanowire width, and this width profile remains almost unchanged with the increase of SW amplitude, both for bulk and edge modes of a nanowire [34]. In this case the development

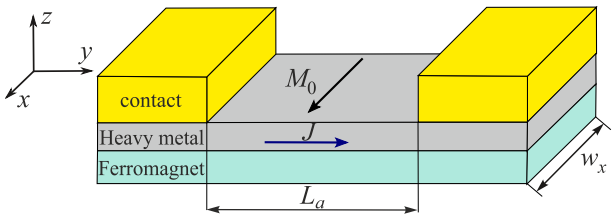

Fig. 1. Sketch of the considered quasi-1D SHO, comprising a ferromagnet–heavy metal nanowire and thick metal contacts, which define the active area between them.

of the magnetization dynamics takes place only along the nanowire length (y coordinate), and is determined by the distribution of bias current density $J(y)$, which exerts STT due to the spin-Hall effect. Below, we assume a rectangular profile of the bias current: $J(y) = J$ within the active region of the length L_a and $J(y) = 0$ outside it. We also assume the static magnetization to be directed along the x direction, that is the most efficient geometry for the SW excitation by the spin-Hall effect. Notes on the influence of the static magnetization direction on the magnetization dynamics will be given below.

The magnetization dynamics in this SHO is studied in the framework of a nonlinear Ginzburg–Landau equation which is derived from the corresponding Landau–Lifshitz equation accounting for linear and first nonlinear ($\sim |b|^3$) terms [22,34]:

$$\frac{\partial b}{\partial t} + (i + \alpha_G)\hat{\Omega} * b + iN |b|^2 b - \sigma J(y)\left(1 - |b|^2\right) b = 0 . \quad (1)$$

Here $b = b(y,t)$ is the complex amplitude of the dynamic magnetization in the excited spin-wave mode, α_G is the effective damping constant, which could be different from the standard Gilbert constant due to the contribution of the spin pumping into a heavy metal layer and/or large precession ellipticity, the parameter N describes the nonlinear frequency shift [36], and the coefficient σ is the spin-transfer torque or spin-Hall efficiency for a STO or SHO, respectively, exact expressions for which is not important for our current work and can be found elsewhere [28,36].

The frequency operator $\hat{\Omega}$ is given by

$$\hat{\Omega} * b \equiv \omega_0 b - \omega_M \lambda_{ex}^2 \frac{\partial^2 b}{\partial y^2} + \frac{\omega_M^2}{2\omega_0} \int G_{yy}(y - y') b(y')\, dy', \quad (2)$$

where $\omega_M = \gamma \mu_0 M_s$, λ_{ex} is the exchange length of the ferromagnet, and ω_0 is the frequency of a spin wave resonance in the linear regime, which is assumed to be constant. A spatial dependence of the ω_0 can be induced, e.g., by the Oersted field of the bias current, and, in the case of a significant nonuniformity of this field, could affect the nature of the excited mode [37]. The last integral term, which was neglected in most of the previous studies, describes the dipole–dipole interaction with G_{yy} being the yy-component of the magnetostatic Green's function for a nanowire geometry [38]. In several previous works the effect of the dipolar interaction on magnetic solitons was considered within a local approximation (as an effective anisotropy) [6]. Attempts to account long-range nature of dipolar interaction were done in [39,40]; however, the approximation made in these works is valid for small-amplitude solitons, which is not the case of solitons excited by STT. In the particular case presented below, rigorous accounting for the dipolar interaction is of a principal importance.

In the following, we present the results of a numerical solution of Eq. (1). As it is usually done in the SW bullet

simulations [41], we have chosen the initial condition in the form of a large-amplitude Gaussian-shape inhomogeneity. The numerical parameters, used in our simulations, are the following: $\omega_0 = 0.25\omega_M$, $N = -0.1\omega_M$, $\lambda_{ex} = 5.5$ nm, $\alpha_G = 0.02$, which are in the range of typical parameters of SHOs based on NiFe/Pt nanowires; the nanowire width was $w_x = 200$ nm, which is used in the expression for the Green's function.

3. Results

A typical dependence of the generation frequency on the bias current, which is obtained in the considered case, is shown in Fig. 2a. The generation starts at a certain threshold $J_{th,1}$, which is determined by the size of the active area and the magnetic parameters of a nanowire. The threshold value is always larger than $J_{th,0} = \Gamma_0 / \sigma$ (where $\Gamma_0 = \alpha_G \omega_0$), which corresponds to the damping compensation for linear SW in the case when the STT is applied to the whole sample (see Eq. (1)). At the threshold $J_{th,1}$, the generation is a single-mode regime, with the frequency lying below the linear SW resonance frequency ω_0. With the increase of the bias current the generation frequency decreases, as it is expected for a negative nonlinear frequency shift. At a certain second threshold value $J_{th,2}$ the generation mode is switched to a different regime. It could be two-mode regime, shown in Fig. 2a, a more complex quasi-periodic regime, or even a generation failure. In this work we are discussing only the first, single-mode generation regime, which is the most important for applications.

The profiles of the excited SW mode are shown in Fig. 2b. At the threshold $J_{th,1}$ the mode has large amplitude and is clearly localized in the vicinity of the active area. Further increase of the bias current leads to the spatial narrowing of the excited mode with simultaneous increase of its amplitude.

All these features of the excited SW mode (the frequency lying below the linear SW resonance, finite mode amplitude at the generation threshold, spatially localized profile) are characteristic for the excitation of self-localized SW soliton (SW bullet mode), and are similar to the corresponding characteristics obtained in the 2D case [22]. The only important difference is the size of the active area, in which we observe the bullet excitation, $L_a = 1$ μm, which is much larger than characteristic sizes of the active area, for which single-bullet mode excitation was reported in the 2D case.

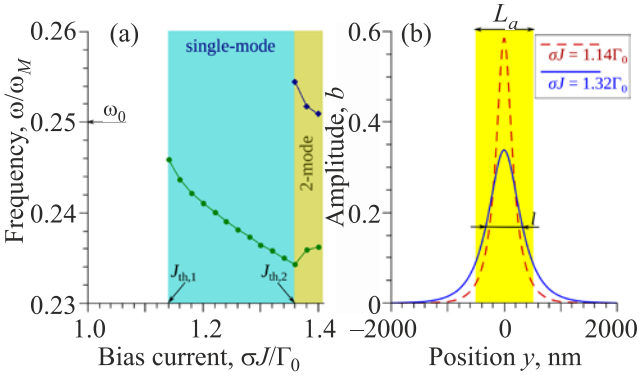

Fig. 2. (Color online) (a) Dependence of the generation frequency of a SHO on the bias current. (b) Profiles of the excited SW mode at the generation threshold $\sigma J_{th,1} = 1.14\Gamma_0$, and at a higher bias current. Calculation parameters: active region length $L_a = 1$ μm, nanowire thickness $h = 5$ nm.

We have systematically studied how the range of bias current, where the single mode generation is realized, evolves with the increase of the active area length L_a (see Fig. 3). First, let us look at the results within the purely exchange approximation, which is achieved by neglecting the integral term in Eq. (2). The excitation threshold of the first bullet mode (lower boundary of the single-mode region) becomes smaller for larger L_a, as one should expect because of a larger in size, and, consequently, smaller in amplitude, bullet can be excited at the threshold. The transition to non-single-mode generation regime also takes place at a smaller bias current in an oscillator with a larger active area, that is a consequence of a smaller exchange energy penalty for the excitation of a second bullet mode, or a more complex nonuniform dynamics. Also, in Fig. 3 we plot the threshold of a linear SW mode excitation, which would have been realized if the nonlinear frequency shift would be zero or positive. In a real experiment, the thermal fluctuations, which are neglected in our simulations, lead to a nonzero thermal level of the linear SWs, and the level of the thermal SWs increases substantially close to the formal threshold of a linear SW mode excitation. This means, that if the thresholds of excitation of

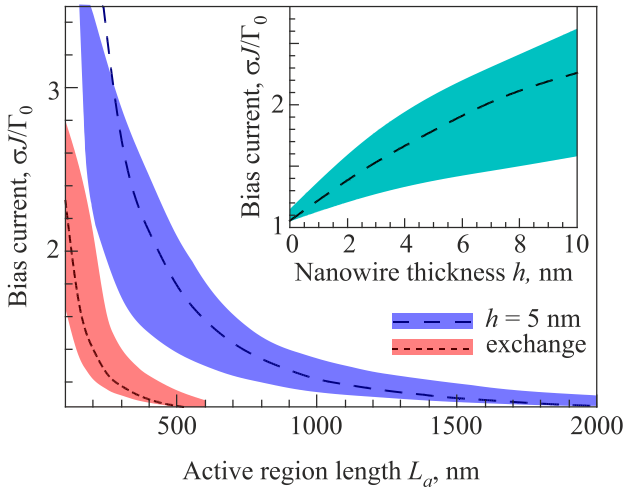

Fig. 3. (Color online) Region of the single-mode generation (shaded area) as a function of the active area length within the purely exchange approximation (red), and within the full dipole-exchange model for the nanowire thickness $h = 5$ nm (blue). Inset shows the region of the single mode generation as a function of the nanowire thickness for the active area length $L_a = 500$ nm. In both panels, dashed lines show the threshold of the linear mode excitation if the nonlinear frequency shift is neglected, $N = 0$.

the bullet and linear SW modes become too close to each other, the thermal noise could break the single-bullet mode generation regime, and a more complex dynamics (e.g., stochastic jumps between different modes, so called "mode hopping" [42]) can be observed. A similar situation takes place if the thresholds of a single-bullet and of a two-bullet mode excitation become close to each other. Single-bullet generation can be observed only if the threshold of its excitation is sufficiently lower than other thresholds. Within the purely exchange approximation this situation takes place if the active area is smaller than 300–400 nm, in full accordance with previous results obtained for the 2D case.

At the same time, if the dipolar interaction is taken into account, all the characteristic thresholds increase substantially (see Fig. 3), and, therefore, the single-bullet mode can be stabilized in a much larger active area, up to $L_a \lesssim 1.5$ μm. By varying the nanowire thickness h we found, that all the thresholds increase with the increase of h (see inset in Fig. 3). This increase of threshold is expected for the excitation of a linear mode, since a larger nanowire thickness corresponds to a larger SW group velocity at low wave numbers. This group velocity is approximately equal to $v_{gr} \approx h\omega_M^2 / (4\omega_0)$ for the considered geometry. The larger group velocity leads to the larger radiation losses which should be compensated by the STT. It is clear from Fig. 3, that the thickness dependence of the bullet excitation threshold follows the same trend as the threshold for the linear mode, meaning that it is also governed by the group velocity increase.

Summarizing this part, we can state, that: (i) dipolar interaction is crucial for the stabilization of the SW bullet mode in large, micron-sized active area of a SHO, and (ii) the amplitude range of existence of the single-bullet mode, as well as the maximum size of the active area in which generation of this mode can be achieved, are mainly determined by the SW group velocity, and increase with the increase of the group velocity. This fact can be explained by a more effective energy flow from the active area when v_{gr} is increased.

It should be noted, that the appearance of dipole-dominated solitons is not trivial, as they do not satisfy the Lighthill criterium $ND < 0$ [35], where $D = \partial^2\omega / \partial k^2$ is the dispersion of the SW group velocity. For the exchange-dominated spectrum $D = 2\omega_M \lambda_{ex}^2 > 0$, and the criterium is satisfied. However, for the dipole-exchange SW spectrum the dispersion is negative ($D < 0$) at low k. We also checked the pure dipolar case (setting $\lambda_{ex} = 0$), for which $D < 0$ in all the range of the SW wave numbers, and the results remain almost the same. Therefore, we can conclude that the dipole-dominated SW bullets are the solitons of a purely dissipative nature and they can exist only in an active medium with a local source of energy pumping, like it happens in the active area of our SHO. In contrast, 1D exchange-dominated SW bullets are not restricted by this limitation. Note, however, that in a conservative 2D case the SW bullets are instable in respect to splitting into multiple solitons.

Now we discuss the properties of the dipole-dominated SW bullets. Their spatial profiles are shown in Fig. 2b. We have found, that the profile of an SW bullet in this case is well-described by the same two-parameter function, i.e., $b(y) = B_0 f(y/l)$, where B_0 is the bullet amplitude, and l is its characteristic width. The normalized function $f(\eta)$ is almost the same for the different values of the bias currents and/or different lengths of the active region. Some differences are present at the bullet "tails", away from the active region. However, a numerical simulation is not a particularly convenient tool to study the small details of the obtained bullet profiles due to the possible numerical errors and the finite size of the simulation area. Rather unexpectedly, the bullet profile is well-described by the function $f(\eta) = 1/\cosh(2.62\eta)$, which is the exact solution for a 1D magnetic soliton in the purely exchange approximation. Some discrepancy with this analytically obtained profile takes place only at the tails, where the dynamic magnetization is small, $b(y) \ll B_0$. Thus, one can use the function $f(\eta) = 1/\cosh(2.62\eta)$ for the analytical estimations of the bullet excitation threshold using the method described in Ref. 22, and expect a reasonably good accuracy. A more rigorous description of the spatial profile of a dipole-dominated bullet, especially at the tails, requires a more detailed analytical consideration.

In the exchange approximation, the SW bullet frequency is related to its amplitude by the expression (recall, that $N < 0$):

$$\omega_{bul} = \omega_0 + NB_0^2 / 2.2 . \qquad (3)$$

The frequency of dipole-dominated bullets follows the same dependence, as shown in Fig. 4a. This fact is not surprising, because this dependence is equivalent to $\omega_{bul} = \omega_0 + N\int |b|^3 dy / \int b dy$, which means that the bullet frequency is fully determined by the nonlinear frequency shift.

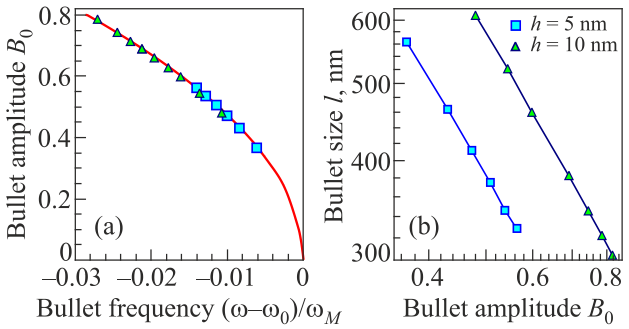

Fig. 4. (a) Dependence of the SW bullet amplitude on the bullet frequency. Points — simulations for $h = 5$ nm and $h = 10$ nm, line — Eq. (3). (b) Bullet size l as a function of its amplitude. Lines are the guides for an eye.

A more interesting is the dependence of the bullet width on its amplitude. The bullet width here is defined as the width at half-maximum of its amplitude, as shown in Fig. 2b. In the exchange approximation one gets $l \sim 1/B_0$. From the numerical simulations we found, that the width of dipole-dominated SW bullets also follows the power-law dependence described by $l = C/B_0^{\beta}$, but the exponent $\beta \neq 1$ (see Fig. 4b and note the log–log scale). For various nanowire thicknesses h and SW resonance frequencies ω_0 we have found that the exponent is in the range $\beta \approx 1.25-1.35$. The coefficient C, naturally, increases with the SW group velocity (i.e. with the increase of the nanowire thickness), meaning that the SW bullets of the same amplitude are wider, if the dipolar interaction is stronger. A more rigorous determination of the localization rules for the dipolar SW bullets requires a detailed analytical model, and lies out of the scope of our current work. Also, note that approximate theory for low-amplitude dipolar solitons yields different exponent $\beta = 2$ [39,40], meaning that typical STT-driven bullets are definitely out of the applicability range of this approximation.

At the end, we would like to discuss the influence of the SHO geometry on the formation of the dipolar SW bullets. As it is shown above, the effect of the dipolar interaction on the SW bullet formation is mostly connected with the dipolar SW group velocity, which significantly depends on the orientation of the nanowire static magnetization in respect to the SW propagation direction. The maximum effect is expected in the case of "Damon–Eshbach" geometry, when the nanowire is magnetized along its width, while the SW propagates along the nanowire length. This case was considered in the above presented calculations.

In the case of a perpendicular magnetization of a nanowire, the formation of dipole-dominated SW bullets is also expected, but it can be realized only for a conventional STO, as the spin-Hall effect does not work in this geometry. The SW group velocity in this case is also positive, $v_{gr} \approx \omega_M h/4$, and for a relatively thick nanowire can be sufficiently large to support the formation of a dipolar SW bullet. In contrast, in the case of a nanowire magnetized along its axis (y direction in Fig. 1), the dipolar SW group velocity becomes negative. Thus, the dipolar interaction does not lead to the additional energy flow from the active area, and, therefore, cannot support large-size SW bullets.

The anisotropy of the SW dispersion in an in-plane magnetized magnetic film explains why in the 2D case only relatively small, exchange-dominated SW bullets were observed. Indeed, for a certain cone of the polar angles ϕ, $[\phi < \phi_0] \cup [(\phi + \pi) < \phi_0]$, where $\phi = 0$ corresponds to the direction parallel to the film static magnetization and ϕ_0 depends on the material parameters and the external bias magnetic field, the SW group velocity is negative. Therefore, in these directions the length of the active area cannot exceed several hundreds of nanometers, as, otherwise, the bullet instability develops in these directions. Since in practically all the experiments the active area of a STO or a SHO was approximately of a circular shape, only in active areas having the size of the order of hundreds of nanometers the stable single-mode SW generation was observed. Judging from our above presented simulations, we expect that if one designs a 2D SHO with an active area elongated along the direction, perpendicular to the static magnetization, an elliptic-shape 2D SW bullet with a micron-scale size in this direction and 100–200 nm size in the perpendicular direction can be formed and stabilized.

4. Conclusions

In conclusion, we studied theoretically the formation and properties of SW bullets in a quasi-1D STO. It is demonstrated that in the 1D case, the dipolar interaction can play a dominant role in the process of the SW bullet formation. In contrast with the exchange-dominated SW bullets [22], the dipole-dominated bullets are purely dissipative solitons can only exist in an active, externally pumped medium. The dipolar interaction can substantially enlarge the characteristic width of the SW bullet, and can make possible a stable single bullet mode excitation in a STO having a relatively large, micron-scale size of the active area. The stabilizing effect of the dipolar interaction scales with the group velocity of the linear SWs at $k \to 0$. The higher is the SW group velocity, the larger is the range of the bias currents corresponding to the single-mode generation for a given length of the active area, and the larger is the maximum length of the active area, in which a stable single-mode generation can be achieved. The spatial profiles of the large-size dipole-dominated dissipative SW bullets are very similar to the profiles of the small-size conservative exchange-dominated SW bullets, and they both demonstrate the same dependence of the bullet frequency on its amplitude. At the same time, the localization law for the dipolar SW bullets $l = C/B_0^{\beta}$ with $\beta \approx 1.25-1.35$ differs from the corresponding law in the exchange-dominated case, where $\beta = 1$. Our results show a way to increase the size of the SHO active area in which a single-mode SW generation can take place, which could be useful in the design of relatively high-power SHO-based generators of microwave signals.

Acknowledgements

This work was supported in part by the NSF of the USA (Grants # EFMA-1641989 and # ECCS-1708982), by the U.S. Air Force Office of Scientific Research under the MURI grant # FA9550-19-1-0307, by the Oakland University Foundation, and by the Ministry of Education and Sciences of Ukraine (project 0118U004007).

1. O. Prokopenko, D. Bozhko, V. Tyberkevych, A. Chumak, V. Vasyuchka, A. Serga, O. Dzyapko, R. Verba, A. Talalaevskij, D. Slobodianiuk, Yu. Kobljanskyj, V. Moiseienko, S. Sholom, and V. Malyshev, *Ukr. J. Phys.* **64**, 888 (2019).

2. A.M. Kosevich, B.A. Ivanov, and A.S. Kovalev, *Nonlinear Magentization Waves. Dynamic and Topological Solitons*, Naukova dumka, Kyiv (1983).
3. O.R. Sulymenko, O.V. Prokopenko, V.S. Tyberkevych, A.N. Slavin, and A.A. Serga, *Fiz. Nizk. Temp.* **44**, 775 (2018) [*Low Temp. Phys.* **44**, 602 (2018)].
4. B.A. Ivanov and A.M. Kosevich, *Sov. Phys. JETP* **45**, 1050 (1977).
5. A.M. Kosevich, B.A. Ivanov, and A.S. Kovalev, *JETP Lett.* **25**, 486 (1977).
6. B.A. Ivanov, A.M. Kosevich, and I.M. Babich, *JETP Lett.* **29**, 714 (1979).
7. A.M. Kosevich, B.A. Ivanov, and A.S. Kovalev, *Phys. Rep.* **194**, 117 (1990).
8. B.A. Kalinikos, N.G. Kovshikov, and A.N. Slavin, *JETP Lett.* **38**, 413 (1983).
9. B.A. Kalinikos, N.G. Kovshikov, and A.N. Slavin, *Phys. Rev. B* **42**, 8658 (1990).
10. K.Yu. Guslienko, *J. Nanosci. Nanotechnol.* **8**, 2745 (2008).
11. R. Antos, Y. Otani, and J. Shibata, *J. Phys. Soc. Jpn.* **77**, 031004 (2008).
12. *Skyrmions. Topological Structures, Properties, and Applications*, J.P. Liu, Z. Zhang, and G. Zhao (eds.), CRC Press, (2016).
13. G. Finocchio, F. Büttner, R. Tomasello, M. Carpentieri, and M. Kläui, *J. Phys. D* **49**, 423001 (2016).
14. A. Fert, N. Reyren, and V. Cros, *Nat. Rev. Mater.* **2**, 17031 (2017).
15. D. Navas, R.V. Verba, A. Hierro-Rodriguez, S.A. Bunyaev, X. Zhou, A.O. Adeyeye, O.V. Dobrovolskiy, B.A. Ivanov, K.Y. Guslienko, and G.N. Kakazei, *APL Mater.* **7**, 081114 (2019).
16. F. Zheng, F.N. Rybakov, A.B. Borisov, D. Song, S. Wang, Z.-A. Li, H. Du, N.S. Kiselev, J. Caron, A. Kovács, M. Tian, Y. Zhang, S. Blügel, and R.E. Dunin-Borkowski, *Nat. Nanotechn.* **13**, 451 (2018).
17. S. Wintz, C. Bunce, A. Neudert, M. Körner, T. Strache, M. Buhl, A. Erbe, S. Gemming, J. Raabe, C. Quitmann, and J. Fassbender, *Phys. Rev. Lett.* **110**, 177201 (2013).
18. J.C. Slonczewski, *J. Magn. Magn. Mater.* **159**, L1 (1996).
19. L. Berger, *Phys. Rev. B* **54**, 9353 (1996).
20. S.I. Kiselev, J.C. Sankey, I.N. Krivorotov, N.C. Emley, R.J. Schoelkopf, R.A. Buhrman, and D.C. Ralph, *Nature* **425**, 380 (2003).
21. G. Bertotti, I. Mayergoyz, and C. Serpico, *Nonlinear Magnetization Dynamics in Nanosystems*, Elsevier (2009).
22. A. Slavin and V. Tiberkevich, *Phys. Rev. Lett.* **95**, 237201 (2005).
23. S. Bonetti, V. Tiberkevich, G. Consolo, G. Finocchio, P. Muduli, F. Mancoff, A. Slavin, and J. Åkerman, *Phys. Rev. Lett.* **105**, 217204 (2010).
24. H. Ulrichs, V.E. Demidov, and S.O. Demokritov, *Appl. Phys. Lett.* **104**, 042407 (2014).
25. M.A. Hoefer, T.J. Silva, and Mark W. Keller, *Phys. Rev. B* **82**, 054432 (2010).
26. S.M. Mohseni, S.R. Sani, J. Persson, T.N. Anh Nguyen, S. Chung, Ye. Pogoryelov, P.K. Muduli, E. Iacocca, A. Eklund, R.K. Dumas, S. Bonetti, A. Deac, M.A. Hoefer, and J. Åkerman, *Science* **339**, 1295 (2013).
27. D.V. Slobodianiuk, O.V. Prokopenko, and G.A. Melkov, *J. Magn. Magn. Mater.* **439**, 144 (2017).
28. A. Giordano, R. Verba, R. Zivieri, A. Laudani, V. Puliafito, G. Gubbiotti, R. Tomasello, G. Siracusano, B. Azzerboni, M. Carpentieri, A. Slavin, and G. Finocchio, *Sci. Rep.* **6**, 36020 (2016).
29. V.E. Demidov, S. Urazhdin, A. Zholud, A.V. Sadovnikov, A.N. Slavin, and S.O. Demokritov, *Sci. Rep.* **5**, 8578 (2015).
30. V.E. Demidov, S. Urazhdin, H. Ulrichs, V. Tiberkevich, A. Slavin, D. Baither, G. Schmitz, and S.O. Demokritov, *Nat. Mater.* **11**, 1028 (2012).
31. V.E. Demidov, S. Urazhdin, E.R.J. Edwards, M.D. Stiles, R.D. McMichael, and S.O. Demokritov, *Phys. Rev. Lett.* **107**, 107204 (2011).
32. Z. Duan, A. Smith, L. Yang, B. Youngblood, J. Lindner, V.E. Demidov, S.O. Demokritov, and I.N. Krivorotov, *Nat. Commun.* **5**, 5616 (2014).
33. K. Wagner, A. Smith, T. Hache, J.-R. Chen, L. Yang, E. Montoya, K. Schultheiss, J. Lindner, J. Fassbender, I. Krivorotov, and H. Schultheiss, *Sci. Rep.* **8**, 16040 (2018).
34. L. Yang, R. Verba, V. Tiberkevich, T. Schneider, A. Smith, Z. Duan, B. Youngblood, K. Lenz, J. Lindner, A.N. Slavin, and I.N. Krivorotov, *Sci. Rep.* **5**, 16942 (2015).
35. M.J. Lighthill, *IMA J. Appl. Math.* **1**, 269 (1965).
36. A. Slavin and V. Tiberkevich, *IEEE Trans. Magn.* **45**, 1875 (2009).
37. R. Verba, *Ukr. J. Phys.* **64**, 947 (2019).
38. K.Y. Guslienko and A.N. Slavin, *J. Magn. Magn. Mater.* **323**, 2418 (2011).
39. A.S. Kovalev, A.M. Kosevich, I.V. Manzhos, and K.V. Maslov, *JETP Lett.* **44**, 222 (1986).
40. A.S. Kovalev, A.M. Kosevich, and I.V. Manzhos, *Sov. Phys. JETP* **67**, 2301 (1988).
41. G. Consolo, B. Azzerboni, G. Gerhart, G.A. Melkov, V. Tiberkevich, and A.N. Slavin, *Phys. Rev. B* **76**, 144410 (2007).
42. G. Consolo, G. Finocchio, G. Siracusano, S. Bonetti, A. Eklund, J. Åkerman, and B. Azzerboni, *J. Appl. Phys.* **114**, 153906 (2013).

Дипольні дисипативні магнітні солітони у квазіодновимірних спін-торк осциляторах

R.V. Verba, V.S. Tiberkevich, A.N. Slavin

Завдяки ефекту спін-трансферу постійний електричний струм, як відомо, може збуджувати у двовимірній феромагнітній плівці обмінні магнітні солітони, які ще називають «спін-хвильовими булетами», за умови від'ємного нелінійного зсуву частоти спінових хвиль. У роботі продемонстровано, що у квазіодновимірному випадку, наприклад, у спін-Холл осциляторі на основі магнітної наносмужки, можливе збу-

дження стійких дисипативних магнітних солітонів, динаміка яких визначається, в першу чергу, магнітодипольною взаємодією. Ці дисипативні магнітні солітони описуються у межах одновимірної моделі автогенератора Гінзбурга–Ландау та мають профіль близький до профілю обмінних солітонів, але виявляють відмінний закон просторової локалізації. Вплив дипольної взаємодії проявляється у можливості стабілізації дисипативного солітона в осциляторі з відносно великою (мікронних розмірів) активною зоною, що сильно відрізняється від двовимірного випадку, у якому утворення спін-хвильових булетів спостерігалось лише у відносно малих активних зонах з типовими розмірами порядку 100 нм. Розглянуто характеристики та можливі застосування таких дипольних спін-хвильових булетів.

Ключові слова: спін-хвильовий булет, спін-торк осцилятор, солітон, магнітодипольна взаємодія.